BIOLOGY OF REPRODUCTION **84,** 775–782 (2011)
Published online before print 8 December 2010.
DOI 10.1095/biolreprod.110.088583

Oxidative Damage Increases and Antioxidant Gene Expression Decreases with Aging in the Mouse Ovary[1]

Jinhwan Lim[3] and Ulrike Luderer[2,3,4]

Division of Occupational and Environmental Medicine, Department of Medicine,[3] and Department of Developmental and Cell Biology,[4] University of California Irvine, Irvine, California

ABSTRACT

Oxidative stress has been implicated in various aspects of aging, but the role of oxidative stress in ovarian aging remains unclear. Our previous studies have shown that the initiation of apoptotic cell death in ovarian follicles and granulosa cells by various stimuli is initiated by increased reactive oxygen species. Herein, we tested the hypothesis that ovarian antioxidant defenses decrease and oxidative damage increases with age in mice. Healthy, wild-type C57BL/6 female mice aged 2, 6, 9, or 12 mo from the National Institute on Aging Aged Rodent Colony were killed on the morning of metestrus. Quantitative real-time RT-PCR was used to measure ovarian mRNA levels of antioxidant genes. Immunostaining using antibodies directed against 4-hydroxynonenal (4-HNE), nitrotyrosine (NTY), and 8-hydroxy-2′-deoxyguanosine (8-OHdG) was used to localize oxidative lipid, protein, and DNA damage, respectively, within the ovaries. TUNEL was used to localize apoptosis. Ovarian expression of glutathione peroxidase 1 (*Gpx1*) increased and expression of glutaredoxin 1 (*Glrx1*), glutathione *S*-transferase mu 2 (*Gstm2*), peroxiredoxin 3 (*Prdx3*), and thioredoxin 2 (*Txn2*) decreased in a statistically significant manner with age. Statistically significant increases in 4-HNE, NTY, and 8-OHdG immunostaining in ovarian interstitial cells and follicles were observed with increasing age. Our data suggest that the decrease in mRNA expression of mitochondrial antioxidants *Prdx3* and *Txn2* as well as cytosolic antioxidants *Glrx1* and *Gstm2* may be involved in age-related ovarian oxidative damage to lipid, protein, DNA, and other cellular components vital for maintaining ovarian function and fertility.

aging, ovary, oxidative stress, reactive oxygen species

INTRODUCTION

The free radical theory of aging has been a driving force in the study of aging since it was first proposed 50 yr ago by Denham Harman [1, 2]. Much of this research has focused on the detrimental roles of reactive oxygen species (ROS) and reactive nitrogen species (RNS), which are formed during cellular metabolism. Aging has been associated with increases in the levels of endogenous ROS and decreases in antioxidant defenses, leading to a wide range of oxidative damage in cell structures, including lipid peroxidation of membranes, enzyme inactivation, protein oxidation, and DNA damage [3–5]. Studies evaluating the role of mitochondria in aging have confirmed that mitochondria are not only a source of cellular energy but also a major source for, and target of, ROS [6, 7]. This research has clearly demonstrated that age-associated oxidative damage differs among organs and cell types [8].

Ovarian aging is characterized by declines in ovarian follicle numbers and in oocyte quality, culminating in reproductive senescence, which in most species occurs long before death [9, 10]. At 13–14 mo of age, the number of ovarian follicles in mice is 10% or less the number of ovarian follicles at 4–5 mo of age [10]. However, few studies have investigated the role of oxidative stress in ovarian aging. Older age was associated with increased ROS and decreased antioxidant levels in oocytes, cumulus cells, and follicular fluid of women undergoing assisted reproduction, and higher ROS levels were associated with worse outcomes [11–13]. These studies suggest that oxidative stress may play a role in the age-related decline in oocyte quality.

Cellular antioxidant defense systems are organized in complex redox circuits with subcellular compartmentation, allowing ROS/RNS to act as signaling molecules at low concentrations [14, 15]. Disruption of these redox circuits results in oxidative stress, even in the absence of free radical-mediated damage [14, 15]. The ovary and oviduct possess antioxidant defenses, including vitamins A, C, and E, as well as the antioxidant tripeptide glutathione (GSH) and ROS-scavenging enzymes, such as superoxide dismutase (SOD), glutathione peroxidase (GPX), catalase (CAT), glutathione *S*-transferase (GST), peroxiredoxin (PRDX), and thioredoxin (TXN) [16–24]. However, relatively little is known about how these ovarian antioxidant defenses change with aging. SOD and GPX enzymatic activities were significantly lower in ovaries of postmenopausal women compared to those of premenopausal women [25]. SOD and CAT expression were lower in cultured granulosa cells collected from 38- to 42-yr-old patients undergoing in vitro fertilization (IVF) compared to those collected from 27- to 32-yr-old IVF patients [11]. In another study of human IVF patients, SOD enzymatic activity and protein levels of SOD1 in cumulus cells surrounding ovulated oocytes decreased significantly with age, and lower levels of SOD activity were associated with unsuccessful IVF outcomes [26]. Oocytes from aged mice were reported to have decreased expression of several antioxidant genes and decreased concentrations of GSH compared to those from young mice [27, 28].

The cellular thiol redox state is controlled by the TXN and the glutaredoxin (GLRX) systems [29]. The antioxidant capacity of GLRX and TXN originates from their ability to use the sulfur (or thiol) group as an electron donor to quench free radicals. GSH acts as a cofactor in the GLRX redox

[1]Supported by NIH grant AG032087 (to U.L.) and the Center for Occupational and Environmental Health, University of California, Irvine. Presented in part at the 92nd Annual Meeting of the Endocrine Society, June 19–22, 2010, San Diego, California.
[2]Correspondence: Ulrike Luderer, Center for Occupational and Environmental Health, University of California, Irvine, 5201 California Avenue, Suite 100, Irvine, CA 92617. FAX: 949 824 2345; e-mail: uluderer@uci.edu

Received: 14 September 2010.
First decision: 14 October 2010.
Accepted: 1 December 2010.

eISSN: 1529-7268 http://www.biolreprod.org
ISSN: 0006-3363

TABLE 1. Body and organ weights and estrous cycle data from 2-, 6-, 9-, and 12-mo-old C57BL/6 female mice.

Age (mo)	Body weight (g)	Paired ovary weight (mg)	Uterus weight (mg)	Cycle length (days)	Leukocytic cytology (%)	Cornified cytology (%)
2	19.5 ± 0.34	11.1 ± 0.80	68.1 ± 10.5	4.7 ± 0.31	49	26
6	22.4 ± 0.6[a]	11.7 ± 0.86	68.6 ± 5.4	4.1 ± 0.08	49	26
9	23.2 ± 0.5[a]	10.7 ± 0.79	88.2 ± 10.9	4.3 ± 0.16	41	30
12	26.0 ± 0.4[a]	12.9 ± 1.62	89.8 ± 4.4	4.1 ± 0.06	50	22

[a] Significantly greater at $P < 0.002$ compared to 2-mo-old by post-hoc Tukey test; N = 6 per age.

balance reactions and in the GSH-dependent enzymatic (GPX, GST, and GLRX) antioxidant defense reactions [30]. A balanced thiol redox state with the aid of the sulfur-redox cycle enzymes, such as glutathione reductase (GSR) and thioredoxin reductase (TXNRD), is important to maintain normal cellular function and cell survival. The disruption of cellular thiol redox homeostasis is a good indicator of oxidative stress in an organism. When the cell is exposed to sustained oxidative stress, the degree of disruption in the balance between oxidizing and reducing conditions increases as a result of the formation and accumulation of disulfides between protein thiols, which can be re-reduced by GLRX or TXN. These alterations of intracellular thiol redox balance may lead to oxidative damage to cellular macromolecules and likely contribute to age-associated diseases [31].

In the present study, we hypothesized that ovarian aging is associated with decreased expression of ovarian antioxidant genes, resulting in oxidative damage to ovarian lipids, proteins, and DNA.

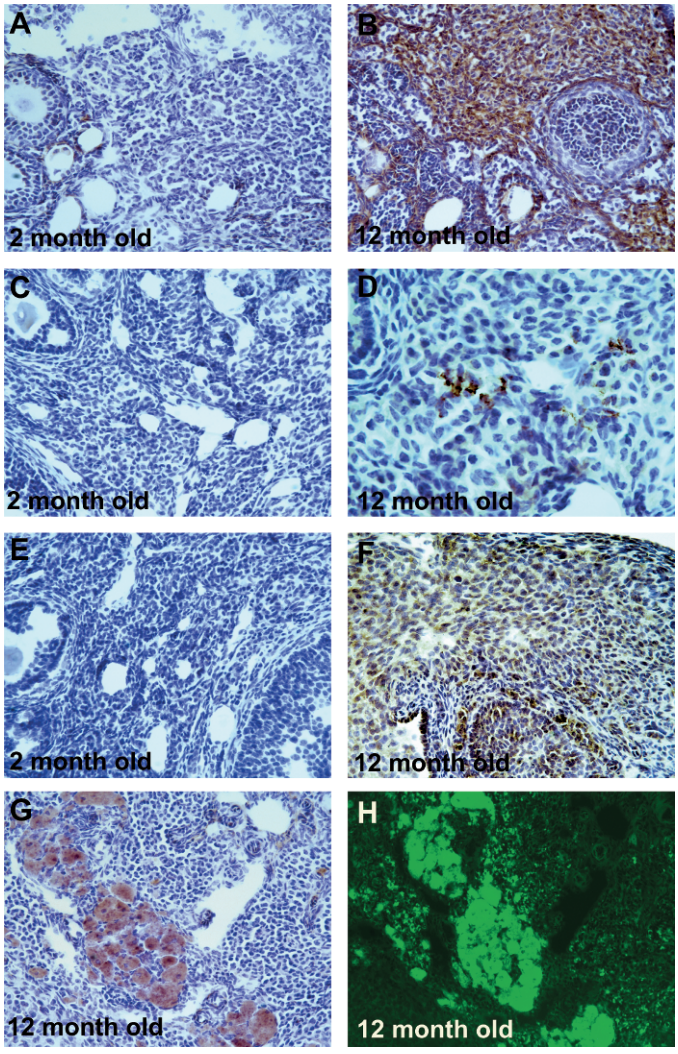

FIG. 1. Effects of aging on oxidative damage in ovarian interstitial cells. Age-related oxidative damage in interstitial cells was scored for immunostaining with oxidative damage markers as described in *Materials and Methods*. Representative images of immunostaining (dark brown) with each oxidative damage marker in interstitial cells are shown: oxidative DNA damage (8-OHdG; **A** and **B**), protein oxidation (NTY; **C** and **D**), and lipid peroxidation (4-HNE; **E** and **F**) in 12-mo-old ovary compared with 2-mo-old ovary. Representative bright-field (**G**) and autofluorescence (**H**) images of the same section from a 12-mo-old ovary immunostained with 8-OHdG and counterstained with hematoxylin are also shown. We verified that the brown areas in **G** are lipofuscin pigments and not 8-OHdG immunostaining by showing that the brown pigmented areas fluoresce yellow/green under blue-light excitation (**H**). Original magnification ×200 (**A**–**C** and **E**–**H**) and ×400 (**D**).

MATERIALS AND METHODS

Materials

All chemicals and reagents were purchased from Fisher Scientific or Sigma-Aldrich unless otherwise noted.

Animals

Female C57BL/6 mice (age, 1, 5, 8, and 11 mo) were purchased from the National Institute on Aging Aged Rodent Resource (n = 6 mice/age). The mice were housed in American Association for the Accreditation of Laboratory Animal Care-accredited facilities, with free access to deionized water and irradiated, soy-free laboratory chow (Harlan Teklad 2919) and a 14L:10D photoperiod. Temperature was maintained at 70–73°F. Mice were allowed to acclimate for 1 wk to the vivarium, after which they were separated into individual cages. The experimental protocols were carried out in accordance with the *Guide for the Care and Use of Laboratory Animals* [32] and were approved by the Institutional Animal Care and Use Committee at the University of California, Irvine.

Estrous Cycling and Ovary Harvest

Estrous cycling in individually housed adult female mice was evaluated every morning for a minimum of 14 days by vaginal cytology [33]. Mice were killed by CO_2 euthanasia on the morning of metestrus. Ovaries and uteri were dissected and weighed. One ovary from each mouse was snap-frozen and stored at −80°C for quantitative real time RT-PCR. The other ovary was fixed for immunohistochemistry for 1–2 h in 4% paraformaldehyde in PBS at 4°C, then cryopreserved in 15% sucrose in PBS for 3–4 h at 4°C, then embedded in Tissue-Tek O.C.T. compound, wrapped in aluminum foil, and stored at −80°C until sectioning.

Quantitative Real-Time RT-PCR

For quantitative real-time RT-PCR, total RNA was extracted from one ovary of each mouse using the Qiagen RNeasy Mini Kit according to the manufacturer's instructions. The quality and quantity of the total RNA were assessed by spectrometry. Purified total RNA (900 ng) was reverse-transcribed to cDNA with Superscript II reverse transcriptase (Invitrogen) using an oligo-$dT_{12–18}$ primer (Invitrogen) after digestion with DNase I (Roche). Twenty nanograms of cDNA were subjected to PCR using gene-specific forward and reverse primers and the Roche SYBR Green RT-PCR reagent (Roche) in 20-μl reaction volumes in duplicate. Gene-specific primers used are listed in Supplemental Table S1 (available online at www.biolreprod.org). Primer

TABLE 2. Distributions of immunostaining for oxidative damage markers and apoptosis in ovarian interstitial cells by age.[a]

	4 HNE[b]		NTY[b]			8-OHdG[b]				TUNEL[c]		
Age group	1	2	0	1	2	0	1	2	3	1	2	3
2 mo												
Observed count	6	0	1	5	0	1	4	1	0	4	2	0
Expected Count	3.8	2.3	0.3	4.2	1.6	0.3	1.0	3.8	1.0	3.3	2.3	0.5
Within age group (%)	100.0	0.0	16.7	83.3	0.0	16.7	66.7	16.7	0.0	66.7	33.3	0.0
6 mo												
Observed count	6	0	0	6	0	0	0	6	0	5	1	0
Expected Count	3.8	2.2	0.3	4.2	1.6	0.3	1.0	3.8	1.0	3.3	2.3	0.5
Within age group (%)	100.0	0.0	0.0	100.0	0.0	0.0	0.0	100.0	0.0	83.3	16.7	0.0
9 mo												
Observed count	2	4	0	4	2	0	0	4	2	2	3	1
Expected Count	3.8	2.2	0.3	4.2	1.6	0.3	1.0	3.8	1.0	3.3	2.3	0.5
Within age group (%)	33.3	66.7	0.0	66.7	33.3	0.0	0.0	66.7	33.3	33.3	50.0	16.7
12 mo												
Observed count	1	5	0	1	4	0	0	4	2	2	3	1
Expected Count	3.8	2.3	0.2	3.5	1.3	0.3	1.0	3.8	1.0	3.3	2.3	0.5
Within age group (%)	16.7	83.3	0.0	20.0	80.0	0.0	0.0	66.7	33.3	33.3	50.0	16.7

[a] Scores of 0, 1, 2, and 3 represent no staining, light staining, localized and dark staining, extensive and dark staining, respectively, for the indicated marker (N = 6 per age).
[b] $P < 0.001$, [c] $P = 0.05$, effect of age by Kendall tau test.

sequences were obtained from previous publications [34, 35] or from Primer Bank (http://pga.mgh.harvard.edu/primerbank/). The PCR amplification of all transcripts was performed on the AB StepOne Plus PCR machine (Applied Biosystems). Transcripts were initially incubated at 95°C for 10 min to activate FastStart Taq DNA polymerase, then underwent 40 cycles of the following program: 95°C for 10 sec, followed by incubation at an average annealing temperature of forward and reverse primers for 30 sec according to the primers used (Supplemental Table S1), and final elongation at 72°C for 10 sec. The quality and identity of each PCR product was determined by melting-curve analysis. Expression of each target gene was calculated by the delta-delta Ct method [36, 37]. All data were normalized to expression of the glyceraldehyde-3-phosphate dehydrogenase (*Gapdh*). Results were also normalized to the expression of *Rn18s*, with essentially the same results. Because the variability in *Rn18s* levels was greater in our hands than the variability in *Gapdh,* we chose to present the results normalized to *Gapdh*.

Immunohistochemistry

For in situ detection of oxidative damage, ovaries were serially sectioned (thickness, 10 μm) using a cryostat. Slides were stored with desiccant at −80°C until immunostaining. For 4-hydroxynonenal (4-HNE) and nitrotyrosine (NTY) immunostaining, antigen retrieval was performed at 95°C for 10 min using citrate buffer, and blocking steps were carried out using the Vectastain ABC kit according to the manufacturer's instructions, with avidin/biotin blocking and 3% hydrogen peroxide blocking steps. Primary antibodies for 4-HNE (catalog no. ALX-210–767; Alexis Biochemicals) [38] and NTY (catalog no. 06–284; Millipore) were utilized at dilutions of 1:500 and 1:50, respectively. Oxidative DNA damage was detected using the Vector M.O.M. immunodetection kit (PK-2200) with a 3% hydrogen peroxide blocking step. Primary antibody for 8-hydroxy-2′-deoxyguanosine (8-OHdG) immunostaining (catalog no. 4354-MC-050; Trevigen) [39] was used at dilution of 1:100. Visualization was accomplished using 3′,3′-diaminobenzidine chromogen substrate (Roche). Sections were counterstained with hematoxylin. The following negative controls were included in every experiment: primary antibody without secondary antibody, secondary antibody without primary antibody, and primary antibody replaced by rabbit immunoglobulin (Ig) G (for 4-HNE and NTY immunostaining) or mouse IgG (for 8-OHdG immunostaining) with secondary antibody. Two or three separate runs of immunostaining were performed for each marker, with at least one slide from each of six ovaries per group per run.

An observer blinded to age performed quantification of oxidatively damaged follicles and interstitial cells. Antral follicles containing three or more (and smaller follicles containing one or more) positive granulosa cells or theca cells per the best cross section were counted. Primordial and primary follicles almost never had positive cells. Interstitial cells were examined for the presence and intensity of immunostaining and scored on a scale from 0 to 3 according to intensity and quantity (0, no staining; 1, light staining; 2, localized and dark staining; 3, extensive and dark staining). Percentages of positive secondary and antral follicles out of the total number of follicles in each follicle type were calculated and used for statistical analyses.

Lipofuscin, an autofluorescent lipid pigment and a marker of aging, in interstitial cells was confirmed by fluorescence (excitation, 450–480 nm; barrier filter, 515 nm) using an Olympus BX60 microscope equipped with a mercury burner and fluorescence filters [40, 41]. Lipofuscin accumulation was distinct in aged groups and was excluded from scoring.

Terminal Deoxynucleotidyl Transferase-Mediated dUTP Nick End-Labeling

Ovarian sections were prepared for TUNEL as for immunostaining. TUNEL was carried out using the In Situ Cell Death Detection Kit, POD (Roche) as previously described [24, 42]. Negative controls without terminal transferase and positive controls treated with DNase I were included in every experiment. Three separate runs of TUNEL were performed, with at least one slide from each of six ovaries per group per run. The numbers of TUNEL-positive and -negative secondary and antral follicles (containing three or more TUNEL-positive granulosa cells or theca cells per the largest cross section) were counted. Primordial and primary follicles almost never had TUNEL-positive cells. The percentages of TUNEL-positive secondary and antral follicles were calculated and used for data presentation and analyses.

Statistical Analyses

Differences in estrous cycles were evaluated using one-way analysis of variance with post hoc Tukey test. Percentages of follicles that stained positively for various markers were subjected to arcsine square root transformation before analysis [43]. The transformed data and ovarian mRNA expression by age were analyzed using general linear regression procedures. Kendall tau correlation analysis was used to determine the changes in interstitial cell damage with age. Data are presented as the mean ± SEM in figures and tables. Statistical analyses were performed using SPSS 16.0 for Mac (SPSS, Inc.).

RESULTS

Estrous Cycling and Reproductive Organ Weights

Female mice of all age groups had regular 4- to 5-day estrous cycles with similar percentages of cornified vaginal cytology, characteristic of estrus, and leukocytic vaginal cytology, characteristic of metestrus and diestrus (Table 1). Body weights increased significantly with age ($P < 0.001$, effect of age by ANOVA). Absolute ovarian and uterine weights (Table 1) as well as ovarian and uterine weights adjusted for body weight (not shown) did not change with age in a statistically significant manner.

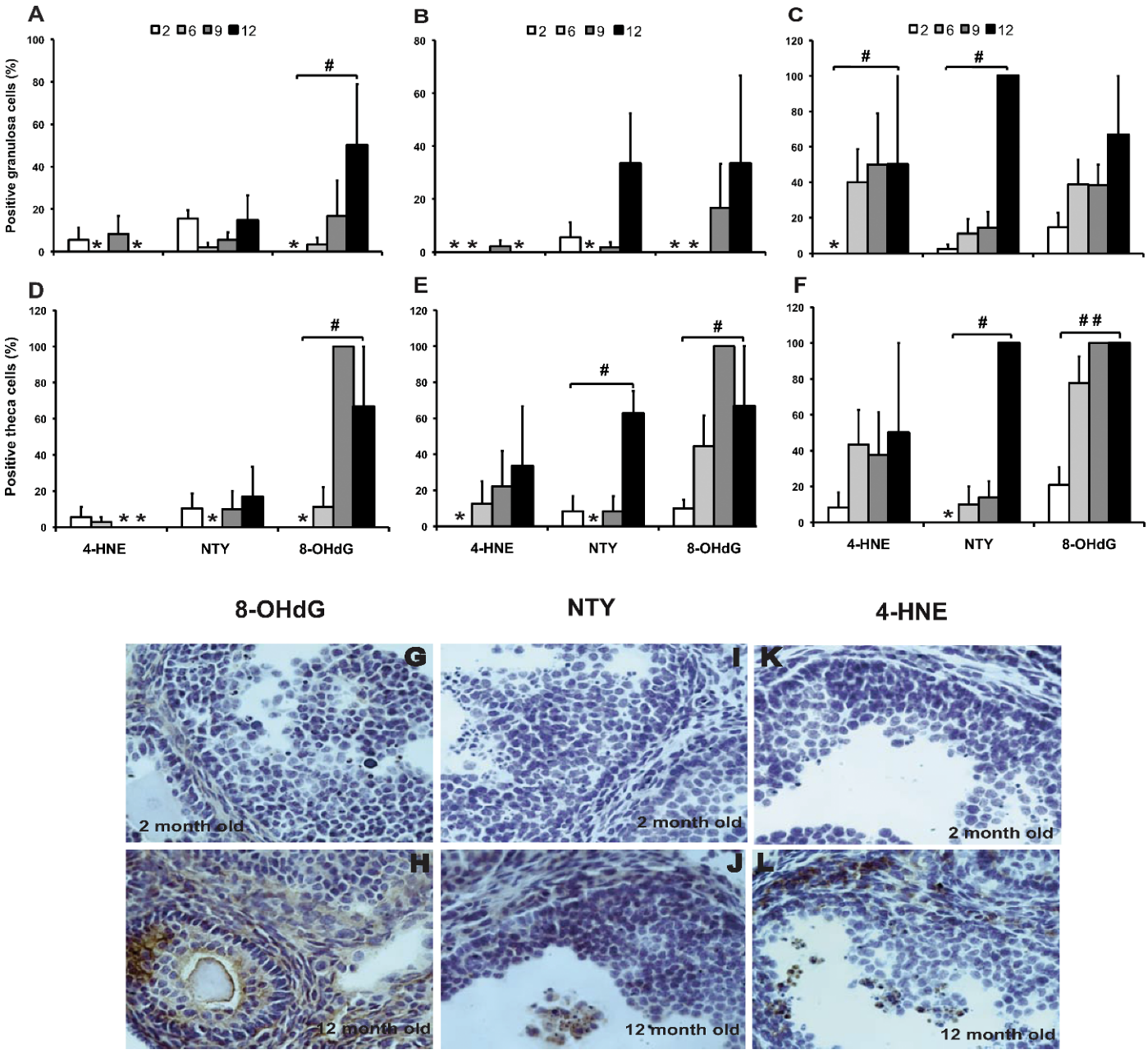

FIG. 2. Effects of aging on ovarian oxidative damage in secondary and antral follicles. The granulosa cells and theca cells of healthy and atretic secondary and antral follicles were scored for immunostaining with oxidative damage markers as described in *Materials and Methods*. Very few atretic secondary follicles were observed. Therefore, the graphs show the percentages of follicles with positive staining for the indicated marker in the granulosa cells of healthy secondary follicles (**A**), healthy antral follicles (**B**), and atretic antral follicles (**C**) or in the theca cells of healthy secondary follicles (**D**), healthy antral follicles (**E**), and atretic antral follicles (**F**). Data are presented as the mean ± SEM of the percentage of follicles with positive staining for the indicated marker from two or three experiments. Asterisks indicate that no follicles scored positive for the given marker and age group. Statistical significance was analyzed using linear regression after arcsine square root transformation ($^{\#}$significant change with age at $P < 0.05$, $^{\#\#}$significant change with age at $P < 0.001$; n = 6 per age). Representative images of immunostaining with each oxidative damage marker in the granulosa and theca cells are shown: DNA damage (8-OHdG; **G** and **H**), protein oxidation (NTY; **I** and **J**), and lipid peroxidation (4-HNE; **K** and **L**) in aged mice (12-mo-old ovary) compared with young mice (2-mo-old ovary). Original magnification ×400.

Age-Related Increase in Oxidative Damage

Oxidative lipid, protein, and DNA damage in interstitial cells increased significantly with age (Fig. 1 and Table 2). In addition, an increase in the levels of apoptosis with aging approached significance ($P = 0.050$) in interstitial cells (Table 2). Accumulation of lipofuscin pigments increased with age and exhibited a distinct interstitial distribution pattern in the 12-mo-old group (Fig. 1G). The identity of the lipofuscin was further confirmed by the demonstration of yellow/green autofluorescence when excited with blue light (Fig. 1H). Characteristic brown lipofuscin deposits were observed even in negative-control slides for which primary antibody was omitted (not shown). DNA damage detected by 8-OHdG immunostaining increased significantly with age in the granulosa cells ($P = 0.013$) and theca cells ($P = 0.002$) of healthy secondary

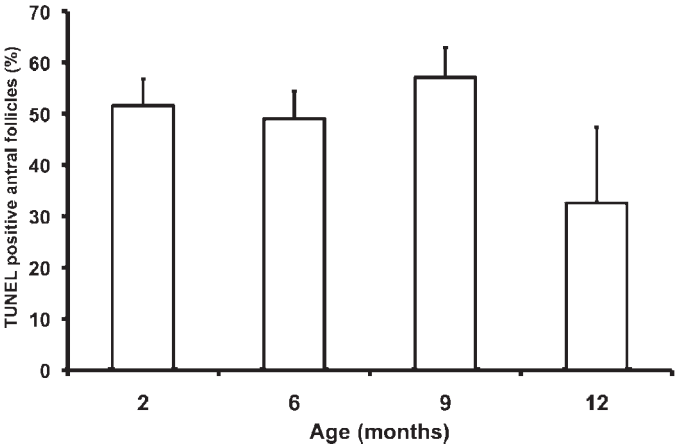

FIG. 3. Effects of aging on apoptosis in antral follicles. TUNEL was performed to detect apoptotic cells as described in *Materials and Methods*. The graph shows the percentage of antral follicles that had TUNEL-positive granulosa cells by age group. Data are presented as the mean ± SEM. The effect of age was not statistically significant ($P = 0.33$ by linear regression; n = 6 per age except for 12 mo, where n = 5).

follicles and in the theca cells of healthy antral follicles ($P = 0.004$) and atretic antral follicles ($P < 0.0001$) and approached significance in the granulosa cells of atretic antral follicles ($P = 0.051$) (Fig. 2). Protein nitration by peroxynitrite, detected by NTY immunostaining, increased with age in the granulosa cells ($P = 0.008$) and theca cells ($P = 0.032$) of atretic antral follicles and in the theca cells of healthy secondary follicles ($P = 0.010$) in a statistically significant manner (Fig. 2). Lipid peroxidation, detected by 4-HNE immunostaining, increased significantly with age in the granulosa cells of atretic antral follicles ($P = 0.014$) (Fig. 2).

Age-Related Changes in Apoptosis

Very few TUNEL-positive primordial, primary, or secondary follicles were observed in any age group. In contrast, a high percentage of antral follicles had TUNEL-positive granulosa cells. The effect of age on the percentages of TUNEL-positive antral follicles was not statistically significant (Fig. 3).

Age-Related Alterations in Antioxidant Gene Expression

Quantitative real-time RT-PCR was used to measure ovarian mRNA levels of the antioxidant genes *Gclc*, *Gclm*, *Sod1, Sod2, Cat, Gpx1, Gpx3*, *Gsr*, *Glrx1, Glrx2*, *Txn1*, *Txn2*, *Txnrd1, Txnrd2, Gsta4, Gstm1, Gstm2, Gstp1, Gstt1, Mgst1*, *Prdx3*, and copper chaperone for SOD *(Ccs)*. The mRNA expression of the mitochondrial antioxidant enzymes *Prdx3* and *Txn2* and the cytosolic antioxidant enzymes *Glrx1* and *Gstm2* decreased gradually with age in a statistically significant manner (Fig. 4). CAT and GPX1 are major cytosolic regulators of H_2O_2 concentration. Expression of *Cat* was unchanged and expression of *Gpx1* increased significantly during aging. In contrast, the mRNA expression of *Prdx3*, the regulator of mitochondrial H_2O_2 concentration and apoptosis, decreased significantly with age (Fig. 4).

DISCUSSION

The present study revealed significant age-related increases in oxidatively damaged lipid, protein, and DNA in ovarian interstitial tissue as well as in granulosa cells and/or theca cells of secondary and antral follicles. The granulosa and theca cells of healthy secondary follicles demonstrated significant age-related increases in DNA oxidation. The theca cells of healthy and atretic antral follicles demonstrated significant age-related increases in protein and DNA oxidation. The granulosa cells of atretic antral follicles demonstrated significant age-related increases in lipid peroxidation, protein oxidation, and oxidative DNA damage. To our knowledge, the present study is the first to investigate age-related changes in markers of oxidative damage in the ovary. We also demonstrated that ovarian expression of genes associated with ovarian thiol redox balance and cellular detoxification of electrophilic compounds—namely *Prdx3, Txn2, Grx1,* and *Gstm2*—was down-regulated during aging. In contrast, ovarian mRNA expression of *Gpx1*, a regulator of cytosolic H_2O_2 concentration, increased with age. These results suggest that age-related alterations of ovarian antioxidant enzyme mRNA expression may contribute to an age-related increase in cellular oxidative damage in the ovary.

Ovarian aging is associated with fertility declines in women and female rodents caused by depletion of ovarian follicles and loss of ovarian cyclicity [10]. In the present study, female mice aged 2 to 12 mo had regular 4- to 5-day estrous cycles with similar percentages of cornified and leukocytic vaginal cytology, consistent with previous reports [9]. Despite regular estrous cycles, we observed significant age-related increases in oxidative damage in the ovaries, and others have reported significant declines in fertility and ovarian follicle numbers at this age in C57BL/6 mice [9, 10]. Our findings support the hypothesis that accumulating oxidative damage may underlie age-related declines in

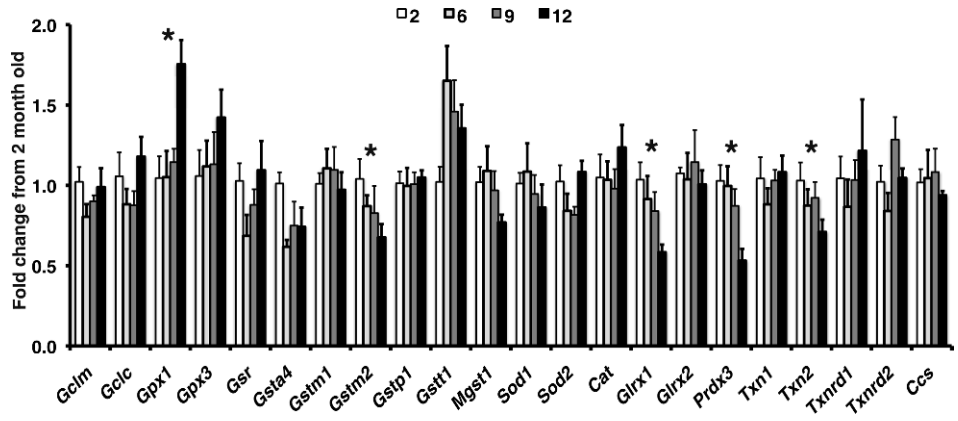

FIG. 4. Changes in ovarian mRNA expression of antioxidant genes during aging. *Gpx1* significantly increased with age ($P = 0.004$ by linear regression), whereas mRNA expression of *Gstm2* ($P = 0.047$), *Glrx1* ($P < 0.001$), *Prdx3* ($P = 0.003$), and *Txn2* ($P = 0.046$) significantly decreased with age. Data are presented as the mean ± SEM. An asterisk indicates significant change with age by linear regression (n = 5–6 per age).

ovarian function. Immunostaining with 8-OHdG increased significantly in an age-related manner in interstitial cells and in the cells of healthy and atretic follicles. A DNA adduct formed from hydroxyl radical attack on guanine residues in DNA, 8-OHdG is the most important and studied DNA lesion. It is a widely accepted biomarker of oxidative DNA damage in biological systems and a potential marker of carcinogenesis [5, 44]. NTY immunostaining, a marker of protein nitration by peroxinitrite, increased with age in ovarian interstitial cells and in the cells of healthy and atretic antral follicles. Oxidative damage to protein is characterized by structural modification of side chains by ROS, including oxidation of sulfhydryl groups, oxidative adducts on amino acid residues near metal-binding sites, cross-linking, unfolding, and protein fragmentation. Direct ROS attack on the amino acid side chains of proline, arginine, lysine, and theonine results in protein carbonyl formation, which eventually changes the tertiary structure of a protein and results in alterations of protein function [4]. We also observed statistically significant increases with age in 4-HNE immunostaining in interstitial cells and in the granulosa cells of atretic antral follicles. 4-HNE is a product of lipid hydroperoxide decomposition. Hydroxyl radicals initiate a free-radical chain reaction and remove a hydrogen atom from one of the carbon atoms in polyunsaturated fatty acids and lipoproteins, causing lipid peroxidation [3, 45]. The damage in membrane phospholipids decreases membrane fluidity, causing severe structural changes, and reduces activity of membrane-bound enzymes, thereby affecting cellular signaling pathways. 4-HNE has been shown to modify mitochondrial proteins, resulting in mitochondrial dysfunction [46].

Others have reported that the effect of aging on antioxidant gene expression varies among different organs and between males and females [28, 47, 48]. One important strength of the present study is that we controlled for estrous cycle stage. Estrous cycle stage is known to affect expression of genes in reproductive, as well as other, tissues. We have previously reported that ovarian *Gclc* and *Gclm* mRNA and protein levels as well as GSH concentrations change with estrous cycle stage in the rat [24, 34]. GSR and TXN expression similarly vary with estrous cycle stage in female reproductive organs [22, 49]. Carcinogen metabolism by the ovary also varies with estrous cycle stage [50]. The only study we are aware of that has compared global gene expression in whole ovaries between young and old females did not take account of estrous cycle stage and compared gene expression in ovaries from 1- and 6-mo-old mice to those from 16- and 24-mo-old mice [51]. By 16–24 mo of age, mouse ovaries are essentially devoid of follicles [10]; therefore, these comparisons cannot provide insight regarding how changes in gene expression might be driving the decline in follicle numbers. Two studies have compared global gene expression in oocytes of young versus old mice [27, 28], and these studies showed decreased expression of several antioxidant genes in germinal vesicle-intact or ovulated oocytes from older mice, including *Sod1, Glrx1, Gclm, Gsr,* GLRX-related protein, and *Txn1*. Our data suggest that down-regulation of antioxidant enzymes during aging, specifically the mitochondrial antioxidant enzymes, may lead to elevated levels of ROS, resulting in oxidative damage in the ovary. Mitochondria-specific antioxidant enzymes, such as PRDX3, TXN2, and TXNRD2, provide a major line of defense against mitochondrial ROS [52]. PRDX3 depletion in cells leads to an increase of H_2O_2 levels in mitochondria [53]. In the present study, we showed that the ovarian expression of *Gpx1* increased significantly during aging, whereas the expression of *Cat* remained unchanged and the expression of *Prdx3* decreased significantly with age. GPX1 is a major cytosolic isoform in mammalian cells that plays a critical role in the protection of cells against oxidative damage by H_2O_2 [54]. PRDX3 is much more abundant in mitochondria and is a major regulator of mitochondrial H_2O_2 concentration and apoptosis [53]. Thus, whereas the age-related increase in *Gpx1* expression may be protective against ROS in the cytosol, the age-related decreases in the expression of *Prdx3* and *Txn2* are consistent with increased susceptibility of mitochondria in aging ovaries to oxidative damage. Our observations that ovarian *Txn2* and *Glrx1* were down-regulated suggest that cellular thiol redox homeostasis is disturbed during ovarian aging, leading to increased vulnerability to oxidative stress. The observed decrease in the expression of *Gstm2*, which plays a role in the cellular detoxification of electrophilic compounds through GSH conjugation and in protection against lipid peroxidation, also suggests a decrease in cellular resistance against oxidative stress. Thus, age-related down-regulation of these cytosolic and mitochondrial antioxidant enzymes and disruption of the cellular thiol redox balance may be associated with increased oxidative damage to mitochondria and other key cellular components vital for maintaining ovarian function during aging.

As has been reported by others, we observed age-related increases in yellow-brown pigment, mainly in the interstitial cells of ovaries. Such age-related accumulations of pigment have been variously referred to as lipofuscins, ceroids, or simply ''age pigments.'' However, the term lipofuscins is more properly reserved for pigments that accumulate in secondary lysosomes of cells during normal aging, whereas ceroids are similar pigments that accumulate during pathological processes [41]. The C57BL/6 strain has a particularly high prevalence (67%) of brown pigment deposition in the ovaries at 1.5 to 2 yr of age [55]. In the present study, we confirmed by autofluorescence that the pigment in the ovaries was lipofuscin. Oxidative stress has been postulated to promote lipofuscin formation in various tissues and cell types, and this has been demonstrated definitively for lipofuscin in the rat retinal pigment epithelium [40, 41]. Our observations of age-related increases in oxidative lipid, protein, and DNA damage in the ovarian interstitial cells provide support for the notion that oxidative stress also promotes the formation of ovarian lipofuscin.

In summary, we have observed age-related increases in oxidative lipid, protein, and DNA damage in ovarian interstitial cells and follicles and decreases in the expression of several ovarian antioxidant genes. These results suggest that intracellular thiol redox homeostasis and cellular antioxidant defense capabilities are diminished during ovarian aging, leading to an increase in oxidative damage in the ovary. Age-related oxidative damage may play a role in the declines in ovarian function that occur with aging.

ACKNOWLEDGMENTS

The authors are grateful to Brooke N. Nakamura, Jesus Banuelos, and Bogdan A. Rau for their assistance with vaginal cytology.

REFERENCES

1. Harman D. Aging: a theory based on free radical and radiation chemistry. J Gerontol 1956; 11:298–300.
2. Harman D. The biologic clock: the mitochondria? J Am Geriatr Soc 1972; 20:145–147.
3. Dean RT, Gieseg S, Davies MJ. Reactive species and their accumulation on radical-damaged proteins. Trends Biochem Sci 1993; 18:437–441.

4. Headlam HA, Davies MJ. Markers of protein oxidation: different oxidants give rise to variable yields of bound and released carbonyl products. Free Radic Biol Med 2004; 36:1175–1184.
5. Orrenius S, Gogvadze V, Zhivotovsky B. Mitochondrial oxidative stress: implications for cell death. Annu Rev Pharmacol Toxicol 2007; 47:143–183.
6. Harman D. The aging process: major risk factor for disease and death. Proc Natl Acad Sci U S A 1991; 88:5360–5363.
7. Wei YH, Lee HC. Oxidative stress, mitochondrial DNA mutation, and impairment of antioxidant enzymes in aging. Exp Biol Med (Maywood) 2002; 227:671–682.
8. Rattan SI. Theories of biological aging: genes, proteins, and free radicals. Free Radic Res 2006; 40:1230–1238.
9. Thung PJ. The senile mouse ovary and its relevance to comparative gerontology. Experientia 1956:74–76 [discussion, 77].
10. Gosden RG, Laing SC, Felicio LS, Nelson JF, Finch CE. Imminent oocyte exhaustion and reduced follicular recruitment mark the transition to acyclicity in aging C57BL/6J mice. Biol Reprod 1983; 28:255–260.
11. Tatone C, Carbone MC, Falone S, Aimola P, Giardinelli A, Caserta D, Marci R, Pandolfi A, Ragnelli AM, Amicarelli F. Age-dependent changes in the expression of superoxide dismutases and catalase are associated with ultrastructural modifications in human granulosa cells. Mol Hum Reprod 2006; 12:655–660.
12. Wiener-Megnazi Z, Vardi L, Lissak A, Shnizer S, Reznick AZ, Ishai D, Lahav-Baratz S, Shiloh H, Koifman M, Dirnfeld M. Oxidative stress indices in follicular fluid as measured by the thermochemiluminescence assay correlate with outcome parameters in in vitro fertilization. Fertil Steril 2004; 82(suppl 3):1171–1176.
13. Das S, Chattopadhyay R, Ghosh S, Goswami SK, Chakravarty BN, Chaudhury K. Reactive oxygen species level in follicular fluid—embryo quality marker in IVF? Hum Reprod 2006; 21:2403–2407.
14. Jones DP. Redefining oxidative stress. Antioxid Redox Signal 2006; 8: 1865–1879.
15. Jones DP. Radical-free biology of oxidative stress. Am J Physiol Cell Physiol 2008; 295:C849–C868.
16. Sato EF, Kobuchi H, Edashige K, Takahashi M, Yoshioka T, Utsumi K, Inoue M. Dynamic aspects of ovarian superoxide dismutase isozymes during the ovulatory process in the rat. FEBS Lett 1992; 303:121–125.
17. Hsieh CH, Tsai SP, Yeh HI, Sheu TC, Tam MF. Mass spectrometric analysis of rat ovary and testis cytosolic glutathione *S*-transferases (GSTs): identification of a novel class-alpha GST, rGSTA6*, in rat testis. Biochem J 1997; 323(pt 2):503–510.
18. Aten RF, Duarte KM, Behrman HR. Regulation of ovarian antioxidant vitamins, reduced glutathione, and lipid peroxidation by luteinizing hormone and prostaglandin F2alpha. Biol Reprod 1992; 46:401–407.
19. Gardiner CS, Salmen JJ, Brandt CJ, Stover SK. Glutathione is present in reproductive tract secretions and improves development of mouse embryos after chemically induced glutathione depletion. Biol Reprod 1998; 59: 431–436.
20. Tilly JL, Tilly KI. Inhibitors of oxidative stress mimic the ability of follicle-stimulating hormone to suppress apoptosis in cultured rat ovarian follicles. Endocrinology 1995; 136:242–252.
21. Mattison DR, Shiromizu K, Pendergrass JA, Thorgeirsson SS. Ontogeny of ovarian glutathione and sensitivity to primordial oocyte destruction by cyclophosphamide. Pediatr Pharmacol (New York) 1983; 3:49–55.
22. Osborne LJ, Tonissen KF, Tang VH, Clarke FM. Expression and localization of thioredoxin in mouse reproductive tissues during the estrous cycle. Mol Reprod Dev 2001; 58:359–367.
23. Leyens G, Verhaeghe B, Landtmeters M, Marchandise J, Knoops B, Donnay I. Peroxiredoxin 6 is up-regulated in bovine oocytes and cumulus cells during in vitro maturation: role of intercellular communication. Biol Reprod 2004; 71:1646–1651.
24. Luderer U, Kavanagh TJ, White CC, Faustman EM. Gonadotropin regulation of glutathione synthesis in the rat ovary. Reprod Toxicol 2001; 15:495–504.
25. Okatani Y, Morioka N, Wakatsuki A, Nakano Y, Sagara Y. Role of the free radical-scavenger system in aromatase activity of the human ovary. Horm Res 1993; 39(suppl 1):22–27.
26. Matos L, Stevenson D, Gomes F, Silva-Carvalho JL, Almeida H. Superoxide dismutase expression in human cumulus oophorus cells. Mol Hum Reprod 2009; 15:411–419.
27. Hamatani T, Falco G, Carter MG, Akutsu H, Stagg CA, Sharov AA, Dudekula DB, VanBuren V, Ko MS. Age-associated alteration of gene expression patterns in mouse oocytes. Hum Mol Genet 2004; 13:2263–2278.
28. Brink TC, Demetrius L, Lehrach H, Adjaye J. Age-related transcriptional changes in gene expression in different organs of mice support the metabolic stability theory of aging. Biogerontology 2009; 10:549–564.
29. Berndt C, Lillig CH, Holmgren A. Thiol-based mechanisms of the thioredoxin and glutaredoxin systems: implications for diseases in the cardiovascular system. Am J Physiol Heart Circ Physiol 2007; 292: H1227–H1236.
30. Hayes JD, McLellan LI. Glutathione and glutathione-dependent enzymes represent a co-ordinately regulated defense against oxidative stress. Free Radic Res 1999; 31:273–300.
31. Halliwell B. Oxidative stress and cancer: have we moved forward? Biochem J 2007; 401:1–11.
32. National Research Council. Guide for the Care and Use of Laboratory Animals. Washington, DC: National Research Council, National Academy of Sciences; 1996.
33. Cooper RL, Goldman JM, Vandenbergh JG. Monitoring of the estrous cycle in the laboratory rodent by vaginal lavage. In: Heindel JJ, Chapin RE (eds.), Female Reproductive Toxicology, vol. 3b. San Diego: Academic Press; 1993:45–55.
34. Tsai-Turton M, Luderer U. Gonadotropin regulation of glutamate cysteine ligase catalytic and modifier subunit expression in rat ovary is subunit and follicle stage specific. Am J Physiol Endocrinol Metab 2005; 289:E391–E402.
35. Xu Z, Chen L, Leung L, Yen TS, Lee C, Chan JY. Liver-specific inactivation of the Nrf1 gene in adult mouse leads to nonalcoholic steatohepatitis and hepatic neoplasia. Proc Natl Acad Sci U S A 2005; 102: 4120–4125.
36. Livak KJ, Schmittgen TD. Analysis of relative gene expression data using real-time quantitative PCR and the 2(-Delta Delta C(T)) method. Methods 2001; 25:402–408.
37. Pfaffl MW. A new mathematical model for relative quantification in real-time RT-PCR. Nucleic Acids Res 2001; 29:e45.
38. Tanaka Y, Aleksunes LM, Goedken MJ, Chen C, Reisman SA, Manautou JE, Klaassen CD. Coordinated induction of Nrf2 target genes protects against iron nitrilotriacetate (FeNTA)-induced nephrotoxicity. Toxicol Appl Pharmacol 2008; 231:364–373.
39. Tsai-Turton M, Nakamura BN, Luderer U. Induction of apoptosis by 9,10-dimethyl-1,2-benzanthracene in cultured preovulatory rat follicles is preceded by a rise in reactive oxygen species and is prevented by glutathione. Biol Reprod 2007; 77:442–451.
40. Brunk UT, Terman A. Lipofuscin: mechanisms of age-related accumulation and influence on cell function. Free Radic Biol Med 2002; 33:611–619.
41. Katz ML, Robison WG Jr. What is lipofuscin? Defining characteristics and differentiation from other autofluorescent lysosomal storage bodies. Arch Gerontol Geriatr 2002; 34:169–184.
42. Lopez SG, Luderer U. Effects of cyclophosphamide and buthionine sulfoximine on ovarian glutathione and apoptosis. Free Radic Biol Med 2004; 36:1366–1377.
43. Pasternack BS, Shore RE. Analysis of dichotomous response data from toxicological experiments involving stable laboratory mouse populations. Biometrics 1982; 38:1057–1067.
44. Kasai H, Crain PF, Kuchino Y, Nishimura S, Ootsuyama A, Tanooka H. Formation of 8-hydroxyguanine moiety in cellular DNA by agents producing oxygen radicals and evidence for its repair. Carcinogenesis 1986; 7:1849–1851.
45. Halliwell B. Antioxidant characterization. Methodology and mechanism. Biochem Pharmacol 1995; 49:1341–1348.
46. Roede JR, Jones DP. Reactive species and mitochondrial dysfunction: mechanistic significance of 4-hydroxynonenal. Environ Mol Mutagen 2010; 51:380–390.
47. Liu R, Choi J. Age-associated decline in gamma-glutamylcysteine synthetase gene expression in rats. Free Radic Biol Med 2000; 28:566–574.
48. Wang H, Liu H, Liu RM. Gender difference in glutathione metabolism during aging in mice. Exp Gerontol 2003; 38:507–517.
49. Kaneko T, Iuchi Y, Kawachiya S, Fujii T, Saito H, Kurachi H, Fujii J. Alteration of glutathione reductase expression in the female reproductive organs during the estrous cycle. Biol Reprod 2001; 65:1410–1416.
50. Bengtsson M, Rydstrom J. Regulation of carcinogen metabolism in the rat ovary by the estrous cycle and gonadotropin. Science 1983; 219:1437–1438.
51. Sharov AA, Falco G, Piao Y, Poosala S, Becker KG, Zonderman AB, Longo DL, Schlessinger D, Ko M. Effects of aging and calorie restriction on the global gene expression profiles of mouse testis and ovary. BMC Biol 2008; 6:24.
52. Pedrajas JR, Miranda-Vizuete A, Javanmardy N, Gustafsson JA, Spyrou G.

Mitochondria of *Saccharomyces cerevisiae* contain one-conserved cysteine type peroxiredoxin with thioredoxin peroxidase activity. J Biol Chem 2000; 275:16296–16301.
53. Chang TS, Cho CS, Park S, Yu S, Kang SW, Rhee SG. Peroxiredoxin III, a mitochondrion-specific peroxidase, regulates apoptotic signaling by mitochondria. J Biol Chem 2004; 279:41975–41984.
54. Kokoszka JE, Coskun P, Esposito LA, Wallace DC. Increased mitochondrial oxidative stress in the Sod2(+/–) mouse results in the age-related decline of mitochondrial function culminating in increased apoptosis. Proc Natl Acad Sci U S A 2001; 98:2278–2283.
55. Maekawa A, Maita K, Harleman JH. Changes in the ovary. In: Mohr U, Dungworth DL, Capen CC, Carton WW, Sundberg JP, Ward JM (eds.), Pathobiology of the Aging Mouse, vol. 1. Washington, DC: ILSI Press; 1996:451–467.